Heterometallic Polymeric Clusters Containing Tetraselenotungstate Anion: One-Dimensional Helical Chain $\{[La(Me_2SO)_8][(\mu\text{-}WSe_4)_3Ag_3]\}_n$ and Cyanide-Bridged Three-Dimensional Cross-Framework $\{[Et_4N]_2[(\mu_4\text{-}WSe_4)Cu_4(CN)_4]\}_n$

Qian-Feng Zhang,[†,‡] Wa-Hung Leung,[‡] Xin-Quan Xin,*[,†] and Hoong-Kun Fun[§]

State Key Laboratory of Coordination Chemistry, Coordination Chemistry Institute, Nanjing University, Nanjing 210093, P. R. China, Department of Chemistry, The Hong Kong University of Science and Technology, Clear Water Bay, Kowloon, Hong Kong, and X-Ray Crystallography Unit, School of Physics, Universiti Sains Malaysia 11800, USM, Penang, Malaysia

Received July 1, 1999

$[PPh_4]_2[WSe_4]$ reacts with an equivalent of $[Ag(MeCN)_4][ClO_4]$ in DMF to afford a linear polymeric cluster $\{[Ph_4P][(\mu\text{-}WSe_4)Ag]\}_n$ (**1**). Treatment of cluster **1** with excess $La(NO_3)_3{\cdot}3H_2O$ in Me_2SO solution resulted in the formation of a helical chain polymeric cluster $\{[La(Me_2SO)_8][(\mu\text{-}WSe_4)_3Ag_3]\}_n$ (**2**). Cluster **2** crystallizes in the monoclinic space group $P2_1/n$ with four formula units in a cell of dimensions $a = 12.7642(5)$ Å, $b = 24.1725(9)$ Å, $c = 19.4012(7)$ Å, and $\beta = 103.546(11)°$. Refinement by full-matrix least-squares techniques gave final residuals $R = 0.0540$ and $R_w = 0.1116$ for 494 variables and 7593 reflections ($F_o^2 > 2.0\sigma(F_o^2)$). The anion $\{[(\mu\text{-}WSe_4)_3Ag_3]\}_n^{3n-}$ in **2** can be described as a butterfly-type $SeWSe_3Ag_2$ basic repeating unit linked through interactions with a Ag atom of one fragment and a Ag atom of another to form an intriguing helical array. The CuCN, KCN, and $[Et_4N]_2[WSe_4]$ reaction system resulted in the formation of a novel three-dimensional cluster $\{[Et_4N]_2[(\mu_4\text{-}WSe_4)Cu_4(CN)_4]\}_n$ (**4**) either in DMF/2-picoline or in solid at 80 °C. Cluster **4** crystallizes in the orthorhombic space group *Fddd* with cell constants $a = 11.090(2)$ Å, $b = 23.206(5)$ Å, $c = 23.910(5)$ Å, and $Z = 8$. Anisotropic refinement with 1510 reflections ($F_o^2 > 2.0\sigma(F_o^2)$) and 82 parameters for all non-hydrogen atoms yielded the values of $R = 0.0428$ and $R_w = 0.0887$. The anion structure of **4** is built up from a WSe_4Cu_4 unit bridged by cyanide ligands to form a three-dimensional cross framework. The air- and moisture-stable polymeric clusters easily decompose into small molecular clusters when treated with ligands such as PPh_3 and pyridine (Py). Cluster **2** exhibits both strong optical absorption and an optical self-focusing effect (effective $\alpha_2 = 2.2 \times 10^{-9}$ m·W^{-1}, $n_2 = 6.8 \times 10^{-15}$ m^2·W^{-1}; examined in a 0.13 mM DMF solution). Cluster **4** shows good photostability in the process of measurement and a large optical limiting effect (the limiting threshold is ca. 0.2 J·cm^{-2}).

Introduction

The chemistry of transition-metal−sulfur clusters[1] has been progressing rapidly owing to their relevance to certain biological and industrial catalyses,[2] rich structural chemistry, and special reactive properties as well as potential application in nonlinear optical materials.[3−5] However, the corresponding chemistry of transition-metal-containing clusters of selenium and tellurium has received less attention than that of the lighter chalcogen elements oxygen and sulfur.[6] Over the past five years there has been increasing interest in this area, partly due to discovery of selenium in some enzymes,[7] and the realization that Se- and Te-containing compounds may have important applications such as precursors for low-band-gap semiconductors, nanomaterials, and nonlinear optics.[8] As part of our interest in thiometalates $[MO_nS_{4-n}]^{2-}$ (M = Mo, W; $n = 0-2$), recently our efforts have

* Corresponding author.
† Nanjing University.
‡ The Hong Kong University of Science and Technology.
§ Universiti Sains Malaysia.

(1) (a) *Transition Metal Sulfur Chemistry: Biological and Industrial Significance*; Stiefel, E. I., Matsumoto, K., Eds.; American Chemical Society: Washington, DC, 1996. (b) Dance, I. G.; Fisher, K. *Prog. Inorg. Chem*. **1994**, *41*, 637. (c) Shibahara, T. *Coord. Chem. Rev*. **1993**, *123*, 73. (d) Lee, S. C.; Holm, R. H. *Angew. Chem., Int. Ed. Engl*. **1990**, *29*, 840.

(2) (a) Howard, J. B.; Low, D. J. *Chem. Rev*. **1996**, *96*, 2965. (b) Kim, J.; Rees, D. C. *Science* **1992**, *257*, 1677. (c) Holm, R. H. *Adv. Inorg. Chem*. **1992**, *38*, 1. (d) Coucouvanis, D. *Acc. Chem. Res*. **1991**, *24*, 1. (e) Wiegand, B. C.; Friend, C. M. *Chem. Rev*. **1992**, *92*, 491.

(3) (a) Huang, Q.; Wu, X.-T.; Sheng, T.-L.; Wang, Q.-M., Lu, J.-X. *Inorg. Chem*. **1995**, *34*, 4931.(b) Ogo, S.; Suzuki, T.; Ozawa, Y.; Isobe, K. *Inorg. Chem*. **1996**, *35*, 6093. (c) Müller, A.; Diemann, E. *Adv. Inorg. Chem*. **1987**, *31*, 89. (d) Sarkar, S.; Mishra, S. B. S. *Coord. Chem. Rev*. **1984**, *59*, 239.

(4) (a) Müller, A.; Diemann, E.; Jostes, R.; Bögge, H. *Angew. Chem., Int. Ed. Engl*. **1981**, *20*, 934. (b) Hadjikyriacou, A. I.; Coucouvanis, D. *Inorg. Chem*. **1987**, *26*, 2400.

(5) (a) Shi, S.; Ji, W.; Tang, S.-H.; Lang. J.-P.; Xin, X.-Q. *J. Am. Chem. Soc*. **1994**, *116*, 3615. (b) Hou, H.-W.; Ye, Y.-R.; Xin, X.-Q.; Liu, J.; Chen, M.-Q.; Shi, S. *Chem. Mater*. **1995**, *7*, 472. (c) Shi, S.; Ji, W.; Xin, X.-Q. *J. Phys. Chem*. **1995**, *99*, 894. (d) Hou, H.-W.; Long, D.-L.; Xin, X.-Q.; Huang, X.-Y.; Kang, B.-S.; Ge, P.; Ji, W.; Shi, S. *Inorg. Chem*. **1996**, *35*, 5363.

(6) (a) Ansari, M. A.; Ibers, J. A. *Coord. Chem. Rev*. **1990**, *100*, 233. (b) Klois, J. W. *Coord. Chem. Rev*. **1990**, *105*, 195. (c) Roof, L. C.; Klois, J. W. *Chem. Rev*. **1993**, *93*, 1037. (d) Huang, S.-P.; Kanatzidis, M. G. *Coord. Chem. Rev*. **1994**, *130*, 509. (e) Arnild, J. *Prog. Inorg. Chem*. **1995**, *43*, 353.

(7) Standtman, T. C. *Annu. Rev. Biochem*. **1990**, *59*, 111.

(8) (a) Dance, I.; Lee, G. *Spec. Publ. R. Soc. Chem*. **1993**, 131. (b) Hirpo, W.; Dhingra, S.; Sutorik, A. C.; Kanatzidis, M. G. *J. Am. Chem. Soc*. **1993**, *115*, 1357. (c) Dhingra, S.; Kanatzidis, M. G. *Science* **1992**, *258*, 1769. (d) Bube, R. H. *Annu. Rev. Mater. Sci*. **1990**, *20*, 19. (e) See any issue of *The Bulletin of the Selenium-Tellurium Development Association*, Grimbergen, Belgium.

10.1021/ic990780g CCC: $19.00
Published on Web 01/07/2000

been largely devoted to exploring nonlinear optical properties of heterobimetallic sulfuric clusters.[5,9] Now we are continuously interested in the heteroselenometalates and their optical nonlinearity; the strategy in this system is directed toward searching for new optical inorganic cluster materials.

Typical convenient precursors for extended heterobimetallic arrays are tetrathiometalates $[MS_4]^{2-}$ (M = Mo, W) and a new half-sandwich trisulfido complex $[(\eta^5\text{-}C_5Me_5)WS_3]^-$, which may react with various metal complexes, resulting in a wide variety of cluster frameworks.[10] Thus, many discrete heterometallic sulfido clusters and a few polymers have been isolated and structurally characterized, for example, the polymeric Mo(W)/Ag/S clusters[11] $[PPh_4]_n[MoS_4Ag]_n$[11a] and $[RPyH]_n[MS_4Ag]_n$ (R = α-Me, β-Me)[11b] (one-dimensional chain), $[H_3NC(CH_2OH)_3\cdot 2DMF]_n[WS_4Ag]_n$ (single chain), $[H_3NC(CH_2OH)\cdot H_2O]_n[WS_4Ag]_n$ (double chain),[11c] $[Ln(DMF)_8]_n[W_4Ag_5S_{16}]_n$ (Ln = Nd, La) (single chain),[11d] $\{[Ca(Me_2SO)_6]_2\}_n[W_4Ag_4S_{16}]_n$ (zigzag chain),[11e] $\{[Nd(Me_2SO)_8]_2\}_n[W_3Ag_3S_{12}]_n$ and $[(\eta^5\text{-}C_5Me_5)WS_3Ag_3(CN)]_n$ (helical chain),[11f,h] and $[(\eta^5\text{-}C_5Me_5)WS_3Ag_2Br]_n$ (ladder chain),[11i] and the polymeric Mo(W)/Cu/S clusters[12] $\{[Me_4N]_2[MoS_4(CuCN)_2]\}_n$ (zigzag-CuCN chain),[12a] $\{[Ph_4P]_2[MoS_4(CuBr)_4]\}_n$ (one-dimensional polymer),[12b] $[WS_4Cu_2]_n$ (binary layer),[12c] $\{[Ph_4P]_2[WS_4(CuSCN)_4]\}_n$ (two-dimensional polymer),[12d] and $\{[Me_4N]_2[WS_4(CuSCN)_4]\}_n$ (three-dimensional network polymer).[12e] In contrast, studies on the reactivities of the corresponding selenides and selenometalate analogues are much less extensively investigated. Müller isolated the first heteroselenometallic silver cluster $[WSe_4(AgPPh_3)_2]$ which was structurally characterized.[13] Ibers has studied interactions of $[WSe_4]^{2-}$ or $[MoSe_4]^{2-}$ with the coinage-metal cations Cu^+, Ag^+, Au^+, and Ni^{2+} and reported successively a number of coinage-metal/$[MSe_4]^{2-}$ (M = Mo, W) complexes with linear, cuboidal, and planar skeletons.[14] One of us synthesized some polynuclear Mo/Cu/Se compounds containing thiolate ligands.[15] But no polymeric structure of this kind of cluster has appeared until now. Herein, we report an initial effort on the inorganic heteroselenometallic polymeric clusters: a one-dimensional helical chain $\{[La(Me_2SO)_8[(\mu\text{-}WSe_4)_3Ag_3]\}_n$ and a cyanide-bridged three-dimensional cross-framework $\{[Et_4N]_2[(\mu_4\text{-}WSe_4)\text{-}Cu_4(CN)_4]\}_n$. Their structural characterizations and NLO properties are also studied in this paper.

Experimental Section

Syntheses. All syntheses were performed in oven-dried glassware under a purified nitrogen atmosphere using standard Schlenk techniques. The solvents were purified by conventional methods and degassed prior to use. All elemental analyses were carried out by the Analytical Center of Nanjing University. $[Ph_4P]_2[WSe_4]$ and $[Et_4N]_2[WSe_4]$ were prepared by an improvement on the literature method.[16] $[Ag(MeCN)_4][ClO_4]$ was prepared from $AgNO_3$ by the reaction with $NaClO_4$ in MeCN solution. CuCN was purchased from Shanghai Reagents Plant and used without further purification.

Preparation of $\{[Ph_4P][(\mu\text{-}WSe_4)Ag]\}_n$ (1). A solution of $[Ag(MeCN)_4][ClO_4]$ (0.186 g, 0.5 mmol) in MeCN (5 mL) was added dropwise to a solution of $[Ph_4P]_2[WSe_4]$ (0.589 g, 0.5 mmol) in DMF (15 mL). The mixture was stirred for a while at room temperature, resulting in a purple-red solution with a small amount of precipitate, and then filtered to afford a brown filtrate. A large amount of black microcrystals of **1** was obtained by slow diffusion of MeCN into the filtrate after 5 days and then washed with MeCN and Et_2O and dried under vacuum, yield (0.398 g, 84%). (Found: C, 29.9; H, 2.16; Se, 32.7. Calcd for $C_{24}H_{20}PSe_4AgW$: C, 30.4; H, 2.11; Se, 33.4.) UV−vis (DMSO, λ_{max}/nm, $10^{-3}\epsilon/M^{-1}\cdot cm^{-1}$): 386 (6.72), 317 (8.91). IR (KBr pellets, cm^{-1}): ν(W−μ-Se), 297.4 (m) and 292.7 (m). Raman (CsI disk, cm^{-1}): ν(Ag−Se), 234.6 (vs); $\delta(WSe_2)$, 142.1 (w). ^{31}P NMR (DMSO-d_6, ppm): δ 24.1. ^{77}Se NMR (DMSO-d_6, ppm): δ 1015.

Preparation of $\{[La(Me_2SO)_8][(\mu\text{-}WSe_4)_3Ag_3]\}_n$ (2). A solution of cluster **1** (0.189 g, 0.2 mmol) in DMSO (10 mL) was added slowly to a solution of $La(NO_3)_3\cdot 3H_2O$ (0.085 g, 0.25 mmol) in DMSO (10 mL) with stirring. The purple-red solution immediately turned dark-brown with a little black precipitate and was subsequently filtered. The filtrate was diffused by MeCN vapor. After a week, black crystals of **2** suitable for X-ray crystallographic analysis were collected and washed with MeCN and EtOH and dried under vacuum, yield (0.084 g, 49%). (Found: C, 7.36; H, 1.82; S, 9.78; Se, 37.1. Calcd for $C_{16}H_{48}O_8S_8Se_{12}LaAg_3W_3$: C, 7.42; H, 1.86; S, 9.90; Se, 36.6.) UV−vis (DMSO, λ_{max}/nm, $10^{-3}\epsilon/M^{-1}\cdot cm^{-1}$): 382 (4.14), 335 (7.84), 304 (9.11). IR (KBr pellets, cm^{-1}): ν(S=O), 1021.4 (vs), 1002.2 (vs), and 989.7 (vs); ν(W−Se_t), 313.6 (s); ν(W−μ-Se) and ν(W−μ_3-Se), 298.5 (m), 288.3 (w), and 280.7 (sh). Raman (CsI disk, cm^{-1}): ν(Ag−Se), 234.8 (vs) and 227.6 (sh); $\delta(WSe_2)$, 162.7 (m) and 145.2 (w). ^1H NMR (DMSO-d_6, ppm): δ 3.31 (CH_3 in Me_2SO). ^{77}Se NMR (DMSO-d_6, ppm): δ 1612, 953, and 792.

Reaction of 1 and PPh_3. A solution of cluster **1** (0.189 g, 0.2 mmol) in DMSO (8 mL) was added to a solution of PPh_3 (0.21 g, 0.8 mmol) and $[PPh_4]\cdot Br$ (0.084 g, 0.2 mmol) in CH_2Cl_2 (15 mL). The mixture was stirred for 2 h at room temperature and then filtered to afford red filtrate. Dropwise addition of *i*-PrOH (10 mL) to the top of the filtrate resulted in the formation of red crystals after the solution was allowed to stand for 3 days. The product was washed with EtOH and Et_2O and dried under vacuum to yield 0.149 g (44.2%). The compound was identified as a cubane-like cluster $[(\mu_3\text{-}WSe_4)Ag_3(PPh_3)_3Br]$ (**3**) by using cell constant determination and elemental analyses. (Found: C, 39.2; H, 2.54; Se, 19.5. Calcd for $C_{54}H_{45}P_3BrSe_4Ag_3W$: C, 38.4; H, 2.66; Se, 18.7.) UV−vis (CH_2Cl_2, λ_{max}/nm, $10^{-3}\epsilon/M^{-1}\cdot cm^{-1}$): 409 (4.57), 338 (8.04), 288 (10.06). IR (KBr pellets, cm^{-1}): ν(W−Se_t), 315.3 (s); ν(W−μ_3-Se), 295.2 (m) and 287.6 (sh). Raman (CsI disk, cm^{-1}): ν(Ag−Se), 235.8 (vs); $\delta(WSe_2)$, 163.5 (s) and 148.2 (w). ^{31}P NMR ($CDCl_3$, ppm): δ 5.47. ^{77}Se NMR ($CDCl_3$, ppm): δ 1674, 1182.

(9) (a) Hou, H.-W.; Xin, X.-Q.; Shi, S. *Coord. Chem. Rev.* **1996**, *153*, 25. (b) Ge, P.; Tang, S.-H.; Ji, W.; Shi, S.; Hou, H.-W.; Long, D.-L.; Xin, X.-Q.; Lu, S.-F.; Wu, Q.-J. *J. Phys. Chem. B* **1997**, *101*, 27.

(10) (a) Müller, A.; Bögge, H.; Schimanski, J. *Inorg. Chim. Acta* **1983**, *69*, 5. (b) Secheresse, F.; Bernes, S.; Robert, F.; Jeannin, Y. *J. Chem. Soc., Dalton Trans.* **1991**, 2875. (c) Lang, J.-P.; Kawagichi, H.; Ohnishi, S.; Tatsumi, K. *Chem. Commun. (Cambridge)* **1997**, 405.

(11) (a) Müller, A.; Jaegermann, W.; Hellmann, W. *J. Mol. Struct.* **1983**, *100*, 559. (b) Lang, J.-P.; Li, J.-G.; Bao, S.-A.; Xin, X.-Q. *Polyhedron* **1993**, *12*, 801. (c) Huang, Q.; Wu, X.-T.; Wang, Q.-M.; Sheng, T.-L.; Lu, J.-X. *Inorg. Chem.* **1995**, *34*, 4931. (d) Huang, Q.; Wu, X.-T.; Wang, Q.-M.; Sheng, T.-L.; Lu, J.-X. *Angew. Chem., Int. Ed. Engl.* **1996**, *35*, 868. (e) Huang, Q.; Wu, X.-T.; Lu, J.-X. *Inorg. Chem.* **1996**, *35*, 7445. (f) Huang, Q.; Wu, X.-T.; Lu, J.-X. *Chem. Commun. (Cambridge)* **1997**, 703. (g) Yu, H.; Zhang, W.-J.; Wu, X.-T.; Sheng, T.-L.; Wang, Q.-M.; Lin, P. *Angew. Chem., Int. Ed.* **1998**, *37*, 2520. (h) Lang, J.-P.; Tatsumi, K. *Inorg. Chem.* **1999**, *38*, 1364. (i) Lang, J.-P.; Kawaguchi, H.; Tatsumi, K. *Inorg. Chem.* **1997**, *36*, 6447.

(12) (a) Müller, A.; Dartmann, M.; Römer, C.; Clegg, W.; Sheldrick, G. M. *Angew. Chem., Int. Ed. Engl.* **1981**, *20*, 1060. (b) Nicholson, J. R.; Flood, A. C.; Garner, C. D.; Clegg, W. *J. Chem. Soc., Chem. Commun.* **1983**, 1179. (c) Pruss, E. A.; Snyder, B. S.; Stacy, A. M. *Angew. Chem., Int. Ed. Engl.* **1993**, *32*, 256. (d) Potvin, C.; Manoli, J.-M.; Sechersse, F.; Marzak, S. *Inorg. Chem.* **1987**, *26*, 4370. (e) Manoli, J.-M.; Sechersse, F.; Marzak, S. *J. Chem. Soc., Chem. Commun.* **1986**, 1557.

(13) Müller, A.; Bögge, H.; Schimanski, J.; Penk, M.; Nieradzik, K.; Dartmann, D.; Krickemyer, E.; Schimanski, J.; Römer, C.; Römer, M.; Dornfeld, H.; Wienböker, U.; Hellmann, W.; Zimmermann, M. *Monatsch. Chem.* **1989**, *120*, 367.

(14) (a) Christuk, C. C.; Ansari, M. A.; Ibers, J. A. *Inorg. Chem.* **1992**, *31*, 4365. (b) Christuk, C. C.; Ibers, J. A. *Inorg. Chem.* **1993**, *32*, 5105. (c) Ansari, M. A.; Chau, C.-N.; Mahler, C. H.; Ibers, J. A. *Inorg. Chem.* **1989**, *28*, 650. (d) Salm; R. J.; Ibers, J. A. *Inorg. Chem.* **1994**, *33*, 4216. (e) Salm, R. J.; Misetic, A.; Ibers, J. A. *Inorg. Chim. Acta* **1995**, *240*, 239.

(15) Hong, M.-C.; Zhang, Q.-F.; Cao, R.; Wu, D.-X.; Chen, J.-T.; Zhang, W.-J.; Liu, H.-Q.; Lu, J.-X. *Inorg. Chem.* **1997**, *36*, 6251.

(16) (a) O'Neal, S. C.; Kolis, J. W. *J. Am. Chem. Soc.* **1988**, *110*, 1971. (b) Zhang, Q.-F.; Hong, M.-C.; Su, W.-P.; Cao, R.; Liu, H.-Q. *Polyhedron* **1997**, *16*, 1433.

Preparation of $\{[Et_4N]_2[(\mu_4\text{-}WSe_4)Cu_4(CN)_4]\}_n$ (4). Method 1. A suspension of CuCN (0.10 g, 1 mmol) and KCN (0.078 g, 1.2 mmol) in 15 mL of DMF/MeOH (v/v: 5/1) was added with stirring to a solution of $[Et_4N]_2[WSe_4]$ (0.167 g, 0.22 mmol) in DMF (8 mL). A red solution with a purple-red solid rapidly formed. Upon addition of 2 mL of 2-picoline solution, the solid precipitate was redissolved. The resultant solution was stirred for 4 h at 45 °C and filtered to afford a red filtrate. Slow vapor diffusion of Et_2O produced after several days X-ray-quality crystals of **4** as black blocks. Yield: (0.187 g, 76%). (Found: C, 22.8; H, 3.44; N, 7,65; Se, 29.5. Calcd for $C_{20}H_{40}N_6Cu_4Se_4W$: C, 21.5; H, 3.60; N, 7.51; Se, 28.3.) UV−vis (DMSO, λ_{max}/nm, $10^{-3}\epsilon/M^{-1}\cdot cm^{-1}$): 396 (3.22), 346 (5.82), 306 (7.28). IR (KBr pellets, cm^{-1}): ν(C≡N), 2118.6 (vs); ν(W−Se), 294.1 (m). Raman (CsI disks, cm^{-1}): ν(C≡N), 2121.1 (vs), ν(Cu−Se), 274.3 (s); $\delta(WSe_2)$, 162.4 (m). ^{1}H NMR (DMSO-d_6, ppm): δ 1.07 (CH_3 in Et_4N), 2.94 (CH_2 in Et_4N).

Method 2. This compound was also synthesized by using the solid state reaction method at a low heating temperature. A well-ground mixture of $[Et_4N]_2[WSe_4]$, CuCN, and KCN (molar ratio of 1:4:8) was heated for 4 h at 80 °C in a Schlenk tube under nitrogen. The raw product was treated by extraction with a DMF/2-picoline (2:1) mixture solvent. A little black precipitate was filtered off, and then the dark-red filtrate was diffused by Et_2O vapor. Dark-black rectangular crystals were obtained in 39% yield. The crystals are stable in air and moisture. Anal. Found: C, 22.1; H, 3.46; N, 7.58; Se, 28.9. Elemental analyses and cell dimension determination showed that the compound was identical to **4** prepared by method 1.

Reaction of 4 and Py. A suspension of cluster **4** (0.168 g, 0.15 mmol) in DMF (10 mL) was added to Py (6 mL). The mixture was stirred for 2 h at 65 °C until the crystalline material was entirely dissolved. Stirring was continued for another 2 h at room temperature, and then the mixture was filtered to afford red filtrate. The filtrate was diffused in a Et_2O vapor atmosphere. A large amount of dark-red microcrystals was obtained after a week. The product was washed with EtOH and Et_2O and dried under vacuum. Yield: 0.154 g (89%). The compound was identified as a WCu_4 core planar cluster $[(\mu_4\text{-}WSe_4)Cu_4(CN)_2(Py)_4]$ (**5**) by using spectroscopic methods and elemental analyses. (Found: C, 37.8; H, 1.71; N, 9.66; Se, 28.1. Calcd for $C_{22}H_{20}N_8Se_4Cu_4W$: C, 38.3; H, 1.74; N, 9.74; Se, 27.5.) UV−vis (DMF, λ_{max}/nm, $10^{-3}\epsilon/M^{-1}\cdot cm^{-1}$): 405 (5.36), 331 (7.92), 294 (8.77). IR (KBr pellets, cm^{-1}): ν(C≡N), 2135.7 (vs); ν(C−N), 1179.2 (s); ν(W−Se), 299.4 (m) and 295.3 (sh). Raman (CsI disks, cm^{-1}): ν(C≡N), 2134.4 (vs), ν(Cu−Se), 276.3 (s); $\delta(WSe_2)$ 163.2 (m). ^{1}H NMR (DMSO-d_6, ppm): δ 8.03, 8.32, and 8.89 (H in Py). ^{77}Se NMR (DMSO-d_6, ppm): δ 742.

Physical Measurements. Electronic absorption spectra were obtained on a Shimadzu UV-3000 spectrophotometer. Infrared spectra were recorded on an FTS-40 spectrophotometer with the use of pressed KBr pellets. Raman spectra were recorded on a Nicolet 910FT-Raman spectrophotometer with the use of pressed CsI disks. NMR spectra were recorded on a Varian Unity-500 spectrometer. Chemical shifts are cited relative to $SiMe_4$ (^{1}H, external), 85% H_3PO_4 (^{31}P, external), and Ph_2Se_2 (^{77}Se, external). Thermogravimeteric analysis was performed by using a Delta TGA7 instrument.

The optical measurements were performed with linearly polarized 7-ns pulses at 532 nm generated from a frequency-doubled Q-switched Nd:YAG laser; the spatial profiles of the pulses were nearly Gaussian after a spatial filter was employed. A DMF solution of compound **2** or **4** was placed in a 1-mm-thick quartz cell for optical limiting measurements. The crystal samples of **2** and **4** are stable toward oxygen, moisture and laser light. The laser beam was focused with a 25-cm focal-length focusing mirror. The radius of the beam circumference was measured to be 30 ± 5 μm (half-width at $1/e^2$ maximum in irradiance). The incident and transmitted pulse energy were measured simultaneously by two energy detectors (Laser Precision Rjp-735) which were linked to a computer by an IEEE interface.[17] The interval between the laser pulses was chosen to be ∼5 s for operational convenience and controlled by the computer. The NLO properties of sample **2** were manifested by moving the sample along the axis of the incident laser beam (*Z*-direction) with respect to the focal point instead of being positioned at its focal point, and an identical setup was adopted in the experiments to measure the *Z*-scan data. An aperture of 0.5 mm radius was placed in front of the detector to assist the measurement of the nonlinear optical refraction effect.

Table 1. X-ray Crystallographic Data for $\{[La(Me_2SO)_8][(\mu\text{-}WSe_4)_3Ag_3]\}_n$ (**2**) and $\{[Et_4N]_2[(\mu_4\text{-}WSe_4)Cu_4(CN)_4]\}_n$ (**4**)

	2	**4**
formula	$C_{16}H_{48}O_8Ag_3Se_{12}W_3La$	$C_{20}H_{40}N_6Cu_4Se_4W$
M	2586.61	1118.43
cryst syst	monoclinic	orthorhombic
space group	$P2_1/n$	*Fddd*
a, Å	12.7642(5)	11.090(2)
b, Å	24.1725(9)	23.206(5)
c, Å	19.4012(7)	23.910(5)
β, deg	103.564(11)	
V, Å^3	5819.1(4)	6153.3(21)
Z	4	8
ρ_{calcd}, g·cm^{-3}	2.952	2.415
λ(Mo Kα), Å	0.710 73	0.710 73
μ, cm^{-1}	15.434	11.198
R_{int}	0.0911	0.0624
R^a	0.0540	0.0428
$R_w{}^b$	0.1116	0.0887

^{a} $R = \sum||F_o| - |F_c||/\sum|F_o|$. ^{b} $R_w = [\sum w(|F_o^2| - |F_c^2|)^2/\sum w|F_o^2|^2]^{1/2}$.

Crystallographic Studies. Well-developed single crystals of **2** and **4** were obtained directly from the preparations as described above. Diffraction data for **2** were collected at 23 ± 1 °C on a Siemens Smart CCD area-detecting diffractometer in the range $2.74° < 2\theta < 56.78°$ by using an ω scan technique. The data reductions were performed on a Silicon Graphics computer station with Smart CCD software. Data collections for **4** were performed at room temperature using the $\omega-2\theta$ scan mode on an Enraf-Nonius CAD4 diffractometer equipped with graphite-monochromated Mo Kα radiation (λ = 0.710 73 Å), and unit cell parameters were based on 25 carefully centered reflections in the range $4.42° < 2\theta < 51.96°$. Absorption correction was applied using ψ scan data. Two structures were solved by direct methods and refined by full-matrix least-squares on F^2 using the SHELXTL 97 (version 5.1) package of crystallographic software.[18] All non-hydrogen atoms were refined anisotropically. The hydrogen atoms were generated and included in the structure factor calculations with assigned isotropic thermal parameters but were not refined. The data processing and structure refinement parameters are summarized in Table 1.

For **2**, the sulfur atoms of three Me_2SO groups and the carbon atoms of two of those three Me_2SO groups were clearly observed disordered. Their site occupancies were each initially set to 0.5, but they were then refined with the restriction that their sum should add up to unity, which resulted in site occupancy values.[19] The weighting scheme used was $\omega = 1/[\sigma^2(F_o^2) + 0.0488P^2 + 0.0000P]$ ($P = (F_o^2 + 2F_c^2)/3$). Final agreement factors were $R(F) = 0.054$ (7593 observed reflections, $F_o^2 > 2\sigma(F_o^2)$) and $R_w = 0.1116$ for 494 parameters. Maximum and minimum residual peaks in the final difference map were 1.708 and −2.018 e·Å^{-3}. For **4**, the weighting scheme used was $\omega = 1/[\sigma^2(F_o^2) + 0.0409P^2 + 0.0000P]$ ($P = (F_o^2 + 2F_c^2)/3$). The final refinement converged to $R = 0.0428$ ($F_o^2 > 2\sigma(F_o^2)$), $R_w = 0.0887$ and $S = 0.959$ on the basis of 82 variables and 1510 independent reflections ($R_{int} = 0.0624$). The largest peak in the final difference map is 1.557 e·Å^{-3}.

(17) (a) Sheik-bahae, M.; Said, A. A.; Wei, T. H.; Hangan, D. J.; Van Stryland, E, W. *IEEE J. Quantum Electron.* **1990**, *26*, 760. (b) Sheik-bahae, M.; Said, A. A.; Van Stryland, E, W. *Opt. Lett.* **1989**, *14*, 955.

(18) Sheldrick, G. M. *SHELXTL-Plus V5.1 Software Reference Manual*; Bruker AXS Inc.: Madison, WI, 1997.

(19) The three sulfur atoms S(5), S(7), and S(8) and the four carbon atoms C(9), C(10), C(13), and C(14) in **2** were treated with disorder. The final refined values of the multiplicities are 0.3 for S(5a), C(9a), and C(10a); 0.7 for S(5b), C(9b), and C(10b); 0.5 for S(7a), S(7b), C(13a), C(13b), C(14a), and C(14b); 0.9 for S(8a) and 0.1 for S(8b).

Results and Discussion

Syntheses and Reactions. When a small amount of a MeCN solution of $[Ag(MeCN)_4][ClO_4]$ was added to a DMF solution of $[PPh_4]_2[WSe_4]$ (molar ratio = 1:1), the purple-red color of the solution darkened immediately. Then the brown filtrate slowly diffused by MeCN to afford the polymeric cluster compound $\{[Ph_4P][(\mu\text{-}WSe_4)Ag]\}_n$ (**1**). The reaction occurred very rapidly, and the resulting compound was insoluble in MeCN and only dissolved in strong polar orangic solvents. Usage of a relatively small amount of $[Ag(MeCN)_4][ClO_4]$ complex is necessary to isolate cluster compound **1** because excess Ag^+ may result in a large amount of Ag_2Se black precipitates. Treatment of **1** in Me_2SO with a slight excess of $La(NO_3)_3 \cdot 3H_2O$ gave a dark brown solution, from which the black block crystals of cluster compound **2** with a one-dimensional helical chain polymeric structure were formed in 49% yield. It has been documented that, in the corresponding tetrathiometalate system, the oxygenphilic Ca^{2+} and Nd^{3+} cations may coordinate the O atoms in Me_2SO solvent to form the larger complex bi- and trivalent cations $[M(Me_2SO)_8]^{n+}$ which can induce the cluster anions in the solution to assemble into some special structural types of polymeric clusters.[11e,f] In the present system, the organic cation $[PPh_4]^+$ can be easily displaced by the larger complex cation $[La(Me_2SO)_8]^{3+}$ as the complementary cation; the latter with the bigger size can stabilize an appropriate size anion. Thus, the original cluster anion $[(\mu\text{-}WSe_4)Ag]^-$ turned to a bigger size cluster anion $[(\mu\text{-}WSe_4)_3Ag_3]^{3-}$ by the self-assembly reaction in the solution. From the results reported here and previously, it is clear that a trend of the dependence of the cluster anion geometric sphere, which may be of novel structures, on the size of the counterion appears to emerge. Larger cations such as $[Ca(Me_2SO)_6]^{2+}$ and $[La(Me_2SO)_8]^{3+}$ effect a polynuclear W/Se(S)/Ag cluster anion polymer (e.g., $[W_4S_{16}Ag_4]^{4-}$ zigzag chain and $[W_3Se_{12}Ag_3]^{3-}$ helical chain)[11e,g] while small ones such as $[PPh_4]^+$ and $[4\text{-}MePyH]^+$ favor a binuclear cluster anion polymer (e.g., $[WS_4Ag]^-$ and $[WSe_4Ag]^-$ linear chain).[11a,b] Such systematic correlation of the counterion size and the geometric sphere of the cluster anion has been observed previously in other systems containing the self-assembly reaction.[20]

For the furtherance of understanding the anion cluster skeleton's transformation from $[(\mu\text{-}WSe_4)Ag]^-$ to $[(\mu\text{-}WSe_4)_3Ag_3]^{3-}$, the course of reaction has been monitored by ^{77}Se NMR spectroscopy. Upon addition of a slight excess of $La(NO_3)_3 \cdot 3H_2O$ in Me_2SO to **1** in Me_2SO, after 30 min, a resonance peak at 1015 ppm weakened and a set of new peaks at 1612, 953, and 792 ppm was found, and the signals are dependent on the reaction time. No change of the ^{31}P NMR signal at 24.01 ppm was observed. In light of this result, it may be suggested that such a complex cation $[La(Me_2SO)_8]^{3+}$ gave rise to the anion cluster skeleton's transformation and the structural variations were undergoing a gradual process by the self-assembly reaction.

An effective way to synthesize heterometallic polymers with transition-metal chalcogenides and copper(I) is to use a copper halide or pseudo-halide fragment.[12b] Müller isolated the first polymeric cluster $\{[Me_4N]_2[MoS_4(CuCN)_2]\}_n$ with an infinite zigzag chain of $\{CuCN\}_\infty$ in a $MeCN/CH_2Cl_2$ reaction solution of $[Me_4N]_2[MoS_4]$ and CuCN in 1:1.5 molar ratio.[12a] With this idea in mind, we have studied the reaction of $[Et_4N]_2[WSe_4]$ with CuCN in the presence of KCN. Unfortunately, the lower solubility of the selenide compounds causes the designed polymeric product to be precipitated in common organic solvents. Ibers has recently reported two W/Se/Cu complexes with a CuCN fragment:[14d] $[PPh_4]_2[(NC)Cu(\mu\text{-}Se)_2W(\mu\text{-}Se)_2Cu(CN)]$ was obtained by the directed combination of the solid reagents followed by dissolution and reaction in MeCN, and $[PPh_4]_2[(CN)Cu(\mu\text{-}Se)_2WSe_2]$ was prepared by the reaction of $[PPh_4]_2[(NC)Cu(\mu\text{-}Se)_2W(\mu\text{-}Se)_2Cu(CN)]$ with excess strong σ-donor ligand PMe_2Ph to form a leaving piece $(PMe_2Ph)_3Cu(CN)$; both cannot induce the formation of heteroselenometallic polymer. We have successfully synthesized a cyanide-bridged three-dimensional framework cluster $\{[Et_4N]_2[(\mu_4\text{-}WSe_4)Cu_4(CN)_4]\}_n$ (**4**) by the using of excess KCN and strong polar solvents DMF and 2-picoline. First, the active fragment $[Cu(CN)_2]^-$ is formed by CuCN and excess KCN in a DMF/MeOH mixture. Then, $[Cu(CN)_2]^-$ reacts with the $[WSe_4]^{2-}$ anion rapidly in DMF solution to cause the product to be precipitated; a little amount of 2-picoline may dissolve all solid in solution. As we expected, 2-picoline only acts as a cosolvent and not a ligand to be ligated to the metal center in the present system.

Alternatively, polymeric cluster **4** can be prepared by the solid state reaction method at a low heating temperature. In the course of the solid state reaction, the color of the starting materials changed gradually from a wine-red to a dark-red, which was accompanied by the evolution of colorless gas. The black precipitate from the extractive solution was analyzed to be selenium powder. Although we have not determined the composition of the gas, the selenium powder is believed to be generated by partial decomposition of $[Et_4N]_2[WSe_4]$. In comparison with the solution reaction, the solid state reaction resulted in a relatively low yield of **4**. One of the reasons is that $[Et_4N]_2[WSe_4]$ is heat-sensitive: on heating, it gradually decomposed to selenium powder and other clusters.[21] A similar finding has been observed for the corresponding sulfuric system.[22] Another important reason is that part of the starting material remained unreacted due to the low interphase reactivity in solids. This notwithstanding, the polymeric cluster **4** of the products obtained from the low-temperature solid state reactions may be partly due to high concentrations of reactants in the well-ground powder state.[23]

As one would expect, the polymeric clusters **1**, **2**, and **4** are dark black air- and moisture-stable solids and they are nonconductors in common organic solvents. However, strong σ-donor ligands, such as PPh_3 and Py, can break the polymeric chain structure into the soluble small molecular clusters. Treatment of excess PPh_3 with **1** in CH_2Cl_2 in the presence of Br^- afforded a complete cubane cluster $[(\mu_3\text{-}WSe_4)Ag_3(PPh_3)_3Br]$ (**3**) (Scheme 1). Similarly, when Py was added to a DMF suspension of **4**, **4** was found to dissolve gradually, and then a WCu_4 core planar cluster $[(\mu_4\text{-}WSe_4)Cu_4(CN)_2(Py)_4]$ (**5**) was isolated (Scheme 2).

Spectral Features. The W−Se stretching modes of the clusters can be identified since they appear as strong and sharp in the low-wavenumber region below 400 cm^{-1}. The terminal $W-Se_t$ absorptions at 314 cm^{-1} for **2** and 315 cm^{-1} for **3** appear

(20) (a) Kanatzidis, M. G.; Huang, S.-P. *Angew. Chem., Int. Ed. Engl.* **1989**, *28*, 1513. (b) Guo, J.; Wu, X.-T.; Zhang, W.-J.; Sheng, T.-L.; Huang, Q.; Lin, P.; Wang, Q.-M.; Lu, J.-X. *Angew. Chem., Int. Ed. Engl.* **1997**, *36*, 2464.

(21) (a) Wardle, R. W. M.; Chau, C.-N.; Ibers, J. A. *J. Am. Chem. Soc.* **1987**, *109*, 1859. (b) Lu, Y.-J.; Ansari, M. A.; Ibers, J. A. *Inorg. Chem.* **1989**, *28*, 4049.

(22) (a) Koniger-Ahlborn, E.; Müller, A. *Angew. Chem., Int. Ed. Engl.* **1975**, *14*, 573. (b) Pan, W.-H.; Harmer, M. A.; Halbert, T. R.; Stefel, E. I. *J. Am. Chem. Soc.* **1984**, *106*, 459.

(23) (a) Li, J.-G.; Xin, X.-Q.; Zhou, Z.-Y.; Yu, K.-B. *J. Chem. Soc., Chem. Commun.* **1991**, 250. (b) Lang, J.-P.; Xin, X.-Q. *J. Solid State Chem.* **1994**, *108*, 118. (c) Lang, J.-P.; Tatsumi, K. *Inorg. Chem.* **1998**, *37*, 6308.

Scheme 1[a]

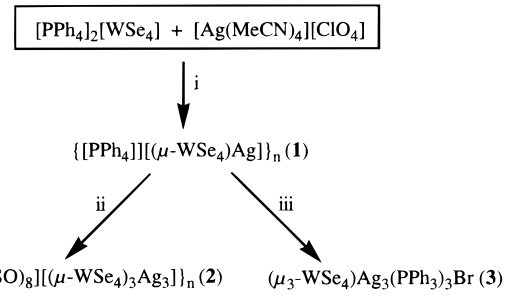

[a] (i) DMF; (ii) $La(NO_3)_3 \cdot 3H_2O/Me_2SO$; (iii) $PPh_3/Et_4N \cdot Br/CH_2Cl_2$.

Scheme 2

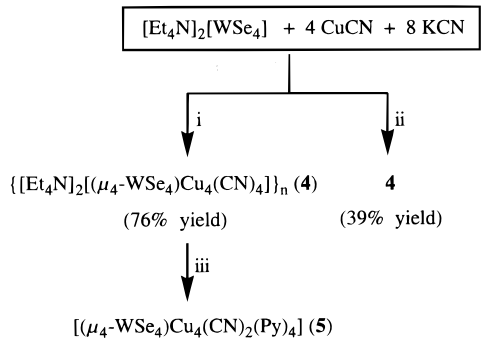

[a] (i) in DMF/2-picoline; (ii) in solid state/80 °C; (iii) Py.

at relatively high wavenumbers compared to the ν(W−Se) absorption at 305 cm^{-1} in $[WSe_4]^{2-}$.[4a,24] However, the bridging W−μ_n-Se (n = 2−4) vibrations in the range 282−300 cm^{-1} are observed at relatively lower wavenumbers from that of $[WSe_4]^{2-}$. Although the M−Se (M = Ag and Cu) vibration modes cannot be easily observed in the lower frequencies of IR spectra, they may be obviously observed in the corresponding frequencies of Raman spectra. Raman spectra of all clusters show two types of strong resonance absorptions in the ranges 220−280 and 140−165 cm^{-1}, respectively. The former may be assigned to the ν(M−Se) (M = Ag and Cu) stretching vibrations, while the latter is due to $\delta(WSe_2)$ bending modes which are similar to those for $[WSe_4]^{2-}$ (163 cm^{-1}). The ν(W−Se) vibration bands cannot be obviously observed in the Raman spectra; a possible reason is that other stronger stretching vibration modes screen the ν(W−Se) modes near the relevant positions. A clear assignment of the bond to ν(C≡N) in both clusters **4** and **5** can be made from a very strong band at 2119 cm^{-1} for **4** and 2136 cm^{-1} for **5**, and the ν(C≡N) itself gives rise to a Raman band showing nearly no resonance enhancement. The stretching vibration of the CN^- anion as bridging coordination in **4** is observed to shift to a relatively lower frequency compared to that as terminal coordination in **5**. The IR spectrum of **2** also shows bands in the range 900−1025 cm^{-1} which can be assigned to the ν(S═O) of the Me_2SO solvent ligands.

Crystals of **1** of suitable quality for X-ray diffraction could not be grown. The structure of **1** however may be deduced from its selenium chemical shift, which is characteristic for a μ-Se atom bonded to silver and tungsten atoms. The chemical shift for **1** is comparable to that of compound (μ-WSe_4)[($PMe_2Ph)_2Ag]_2$ with a similar selenium environment.[14a] The ^{31}P NMR spectrum for **1** shows a singlet at 24.01 ppm, which arises from a $[PPh_4]^+$ cation. The previous results reported by Ibers mapped out that the bridging Se atoms are shielded and the terminal Se atoms are deshielded relative to the Se nuclei in the symmetric anion $[WSe_4]^{2-}$ (δ = 1235 ppm).[25] As expected, three peaks at 1612, 953, and 792 ppm were found in the ^{77}Se NMR spectrum of **2**, which are assigned to the terminal Se, the bridging μ-Se, and μ_3-Se, respectively. Similarly, the ^{77}Se NMR spectrum of **3** shows two peaks at 1674 and 1182 ppm which may be assigned to the terminal and the bridging Se atoms, respectively. Interestingly, compared with chemical shifts of the μ_3-Se atoms in **2** and **3**, the μ_3-Se resonance in **3** is more downfield than that in **2**. This observation indicates that strong σ-donor ligand PPh_3 causes the electron density to transfer from the $[Ag(PPh_3)]^+$ fragments toward the Se_b centers. Attempts to determine the ^{77}Se NMR data for **4** were unsuccessful because of its much lower solubility in polar organic solvents. The ^{77}Se NMR spectrum of **5** shows a broad singlet at 742 ppm which is attributable to the μ_4-Se ligand.

The electronic absorption spectra for clusters **1**−**5** show intense bands in the UV region with weaker bands in the visible region. The patterns for both intense and weaker bands may be ascribed to the internal charge-transfer transitions of the $[WSe_4]^{2-}$ moiety. The absorption bands for clusters **1**−**5** are at higher energies than those for the free $[WSe_4]^{2-}$ anion, as in the parallel sulfide chemistry.[26]

Crystal Structures. Since high-quality single crystals were obtained for **2**, an X-ray diffraction analysis was carried out, revealing that **2** is composed of noninteracting $[La(Me_2SO)_8]^{3+}$ cations and $[(\mu\text{-}WSe_4)_3Ag_3]^{3-}$ macroanions. Although a similar structure has been seen previously in $\{[Ln(Me_2SO)_8][(\mu\text{-}MS_4)_3Ag_3]\}$ (Ln = Nb, La; M = W, Mo),[11f,g] the current arrangement appears to be the first example of a polymeric cluster with $[WSe_4]^{2-}$. The macroanions are infinite one-dimensional chains running parallel to the monoclinic symmetric axis. The basic repeating unit is a butterfly-type $SeWSe_3Ag_2$ containing the bridging μ-WSe_4^{2-} group, which is linked through interactions with a Ag atom of one fragment and a Ag atom of another to form an intriguing helical array of the repeating $[(\mu\text{-}WSe_4)_3Ag_3]^{3-}$ cluster units. Figure 1 represents the packing of the $\{[(\mu\text{-}WSe_4)_3Ag_3]\}_n^{3n-}$ chain in the unit cell with the $[La(Me_2SO)_8]^{3+}$ ions acting as spacers. Figure 2 shows a view of an individual chain which may be thought of as a corrugated ribbon. This chain is made up of two sets of helices which alternatively propagate along the chain. The larger trivalent cations $[La(Me_2SO)_8]^{3+}$ are arrayed among the anionic helical chains and well separated from each other and the anionic chains. Each La(III) atom is coordinated by O atoms of eight Me_2SO molecules. The average La−O bond length of 2.492(9) Å and the O−La−O angles ranging from 68.4(4)° to 147.3(3)° are in the expected ranges (Table 2). All of the W atoms are tetrahedral within error (Se−W−Se angles varying from 106.43(6)° to 114.26(5)°, the mean error and maximum error being 2.42° and 7.83°, respectively). W atoms are more distorted than those for other known $[MSe_4]^{2-}$ (M = Mo, W) derivatives,[27,28] especially for the copper cluster compounds.[14,15] The average Se_t−W−Se_b angle, which is ca. 4.0° more acute than the average Se_b−W−Se_b angle, is similar to that in the butterfly-like silver cluster $\{WAg_2Se_3(C_5H_5NS)\}(PPh_3)_3(Se) \cdot CH_2Cl_2$,[27] but it is different from

(24) Wardle, R. W. M.; Mahler, C. H.; Chau, C.-N.; Ibers, J. A. *Inorg. Chem.* **1988**, *27*, 2970.

(25) Wardle, R. W. M.; Bhaduri, S.; Chau, C.-N.; Ibers, J. A. *Inorg. Chem.* **1988**, *27*, 1747.

(26) Gheller, S. F.; Hambley, T. W.; Rodgers, J. R.; Brownlee, R. T. C.; O'Connor, M. J.; Snow, M. R.; Wedd, A. G. *Inorg. Chem.* **1984**, *23*, 2519.

(27) Wang, Q.-M.; Wu, X.-T.; Huang, Q.; Sheng, T.-L.; Lin, P. *Polyhedron* **1997**, *16*, 1439.

(28) (a) Ansari, M. A.; Bollinger, J. C.; Christuk, C. C.; Ibers, J. A. *Acta Crystallogr.* **1994**, *C50*, 869. (b) Du, S.-W, Wu, X.-T.; Lu, J.-X. *Polyhedron* **1994**, *12*, 841.

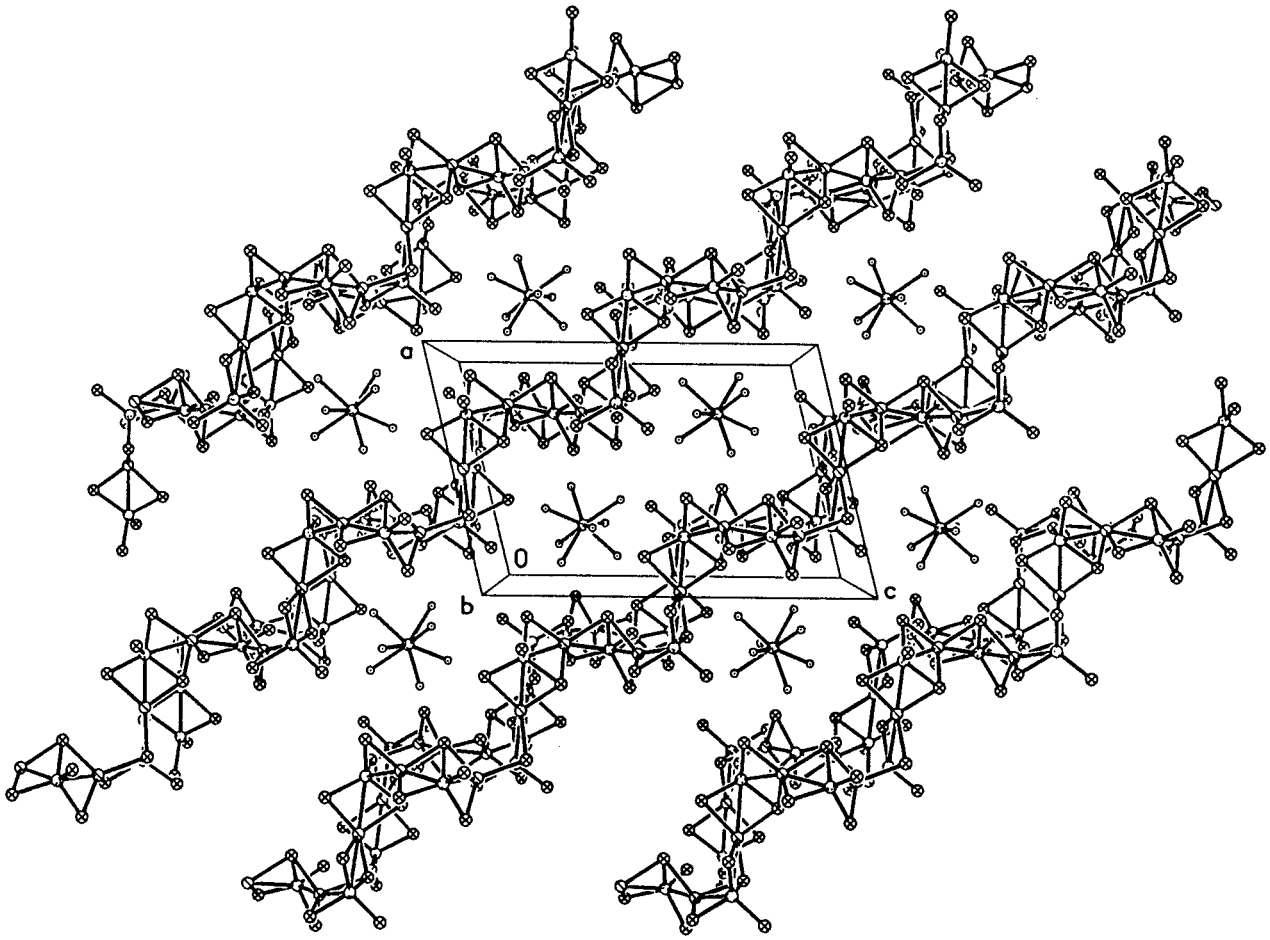

Figure 1. ORTEP representation of the packing arrangement of $[(\mu\text{-}WSe_4)_3Ag_3]_n^{3n-}$ chains in the monoclinic lattice of **2**. The SMe_2 groups in Me_2SO were omitted for clarity.

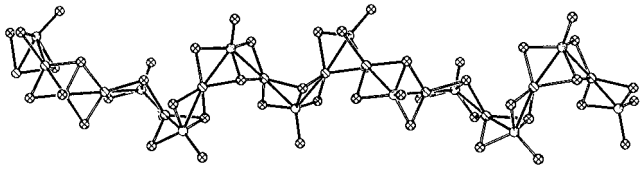

Figure 2. View of a $[(\mu\text{-}WSe_4)_3Ag_3]\}_n^{3n-}$ chain, in **2**, four unit cells long as drawn by ORTEP with 50% displacement ellipsoids.

those in the cubane-like silver clusters $\{WAg_3Se_3I\}(PR_3)_3(Se)$ (R_3 = Ph_3, Me_2Ph).[28] In the Se_b-W-Se_b angles, the angles involving μ_3-Se atoms are obviously bigger than those involving μ-Se atoms. The geometry about the Ag atoms may be described as highly distorted tetrahedral, with angles from 92.71(6)° to 125.65(6)°. Interestingly, a big deviation of the W−Ag−W angles (159.51(4)°, 167.60(4)°, and 178.47(5)°) is found in the helical chain, while a relatively small deviation appears among the Ag−W−Ag angles (82.81(3)°, 85.49(3)°, and 87.15(3)°). This may infer that two μ-Se and two μ_3-Se atoms from different μ-WSe_4^{2-} anions bonded to Ag atoms can result in a butterfly-type $SeWSe_3Ag_2$ unit to develop in spirals and further to form a helical chain.

The W−Se bond lengths similarly fall into three categories: the W−Se_t, W−μ-Se, and W−μ_3-Se bond distances are 2.2840(16), 2.3357(14), and 2.3744(13) Å, respectively. The average W−Ag distance of 3.0038(12) Å is close to those observed in $\{WAg_2Se_3(C_5H_5NS)\}(PPh_3)_3(Se)\cdot CH_2Cl_2$, (average 3.014(2) Å)[27] and in $\{WAg_3Se_3I\}\{[PMe_2Ph]_3(Se)\}$ (average 2.976(1) Å)[28a] and may be a manifestation of a very weak W(VI)−Ag(I) interaction. Bond lengths for the Ag and Se atoms are similar to those reported for analogous clusters[13,27,28] and are comparable to those in Ag/Se compounds, such as $[(Ph_4P)AgSe_4]_n$ (2.545(2)−2.672(2) Å),[29a] $Ag_4(\mu\text{-dppm})_4(\mu_4\text{-Se})][BF_4]_2$ (dppm = bis(diphenylphosphino)methane) (2.613(1)−2.622(1) Å),[29b] $Ag_{11}Se(Et_2NCS_2)_9$ (2.656(4) Å),[29c] and $Ag_{112}Se_{32}(SeBu)_{48}(P\text{-}n\text{-}Bu_3)_{12}$ (2.544(6)−2.726(6) Å).[29d]

The crystal structure of **4** consists of well-separated cations and anions. The framework of the polymeric anion, as shown in Figure 3, is constructed from a WSe_4Cu_4 unit bridged by cyanide ligands. Selected bond distances and angles are collected in Table 3. Each W atom of the structure is at the center of an essentially tetrahedral WSe_4 unit in which the W−Se bond lengths are all quite similar. Four edges of the WSe_4 tetrahedron are coordinated by Cu atoms with W−Cu distances ranging from 2.850(2) to 2.907(2) Å; these values are obviously long compared with those reported previously.[30] In the WCu_4 core, five metal atoms are entirely coplanar, with Cu−W−Cu angles of 180° concerning the two mutually trans Cu atoms, which forms an ideal crystallographic D_{2d} symmetry for the WSe_4Cu_4 aggregate. Four Cu atoms have distorted tetrahedral geometries, of which each of the two sets of trans Cu atoms has pieces of a $CuSe_2N_2$ or $CuSe_2C_2$ unit. Those two kinds of tetrahedra are

(29) (a) Kanatzidis, M. G.; Huang, S.-P. *J. Am. Chem. Soc*. **1989**, *111*, 761. (b)Yam, V. W. W.; Lo, K. K. W.; Wang, C. R.; Chueng, K. K. *Inorg. Chem.* **1996**, *35*, 5116. (c) Zhang, Q.-F.; Cao, R.; Hong, M.-C.; Su, W.-P.; Liu, H.-Q. *Inorg. Chim. Acta* **1998**, *277*, 171. (d) Fenske, D.; Zhu, N.-Y.; Langetepe, T. *Angew. Chem., Int. Ed.* **1998**, *37*, 2640.
(30) (a) Christuk, C. C.; Ansari, M. A.; Ibers, J. A. *Angew. Chem., Int. Ed. Engl.* **1992**, *31*, 1477. (b) Zhang, Q.-F.; Raj, S. S. S.; Fun, H.-K.; Xin, X.-Q. *Chem. Lett.* **1999**, 619.

Table 2. Selected Bond Distances and Angles in **2**[a]

Bond Distances (Å)			
W(1)−Se(1)	2.2732(17)	W(1)−Se(2)	2.3329(17)
W(1)−Se(4)	2.3450(13)	W(1)−Se(3)	2.3737(13)
W(1)−Ag(3)	2.9737(13)	W(1)−Ag(1)	2.9823(11)
W(2)−Se(7)	2.2892(14)	W(2)−Se(8)	2.3299(13)
W(2)−Se(5)	2.3352(15)	W(2)−Se(6)	2.3738(13)
W(2)−Ag(1)	3.0196(11)	W(2)−Ag(2)	3.0231(11)
W(3)−Se(12)	2.2895(17)	W(3)−Se(9)	2.3341(14)
W(3)−Se(11)	2.3372(14)	W(3)−Se(10)	2.3758(12)
W(3)−Ag(3)[a]	2.9974(13)	W(3)−Ag(2)	3.0266(11)
Ag(1)−Se(5)	2.5832(16)	Ag(1)−Se(4)	2.5968(16)
Ag(1)−Se(3)	2.6570(16)	Ag(1)−Se(6)	2.6647(17)
Ag(2)−Se(8)	2.6214(18)	Ag(2)−Se(9)	2.6346(16)
Ag(2)−Se(6)	2.6415(15)	Ag(2)−Se(10)	2.6468(17)
Ag(3)−Se(11)[b]	2.5694(18)	Ag(3)−Se(10)[b]	2.6405(16)
Ag(3)−Se(3)	2.6533(18)	Ag(3)−Se(2)	2.708(2)
Ag(3)−W(3)[b]	2.9974(13)	Se(10)−Ag(3)[a]	2.6406(16)
Se(11)−Ag(3)[a]	2.5694(18)		

Bond Angles (deg)			
Se(1)−W(1)−Se(2)	109.17(8)	Se(1)−W(1)−Se(4)	108.05(6)
Se(2)−W(1)−Se(4)	107.78(6)	Se(1)−W(1)−Se(3)	106.43(6)
Se(2)−W(1)−Se(3)	111.03(6)	Se(4)−W(1)−Se(3)	114.26(5)
Se(1)−W(1)−Ag(3)	147.37(6)	Se(2)−W(1)−Ag(3)	59.92(5)
Se(4)−W(1)−Ag(3)	104.58(4)	Se(3)−W(1)−Ag(3)	58.21(4)
Se(1)−W(1)−Ag(1)	114.94(6)	Se(2)−W(1)−Ag(1)	135.84(5)
Se(4)−W(1)−Ag(1)	56.84(4)	Se(3)−W(1)−Ag(1)	58.16(4)
Ag(3)−W(1)−Ag(1)	82.81(3)	Se(7)−W(2)−Se(8)	107.88(6)
Se(7)−W(2)−Se(5)	106.92(6)	Se(8)−W(2)−Se(5)	107.84(6)
Se(7)−W(2)−Se(6)	107.38(6)	Se(8)−W(2)−Se(6)	113.76(5)
Se(5)−W(2)−Se(6)	112.74(5)	Se(7)−W(2)−Ag(1)	131.16(5)
Se(8)−W(2)−Ag(1)	120.78(4)	Se(5)−W(2)−Ag(1)	55.94(4)
Se(6)−W(2)−Ag(1)	57.74(4)	Se(7)−W(2)−Ag(2)	128.04(5)
Se(8)−W(2)−Ag(2)	56.89(4)	Se(5)−W(2)−Ag(2)	124.98(4)
Se(6)−W(2)−Ag(2)	57.10(4)	Ag(1)−W(2)−Ag(2)	85.49(3)
Se(12)−W(3)−Se(9)	107.27(6)	Se(12)−W(3)−Se(11)	106.94(6)
Se(9)−W(3)−Se(11)	108.05(6)	Se(12)−W(3)−Se(10)	107.39(6)
Se(9)−W(3)−Se(10)	114.16(5)	Se(11)−W(3)−Se(10)	112.66(5)
Se(12)−W(3)−Ag(3)[a]	130.33(5)	Se(9)−W(3)−Ag(3)[a]	122.23(5)
Se(11)−W(3)−Ag(3)[a]	55.95(4)	Se(10)−W(3)−Ag(3)[a]	57.48(4)
Se(12)−W(3)−Ag(2)	126.65(5)	Se(9)−W(3)−Ag(2)	57.13(4)
Se(11)−W(3)−Ag(2)	126.35(5)	Se(10)−W(3)−Ag(2)	57.16(4)
Ag(3)[a]−W(3)−Ag(2)	87.15(3)	Se(5)−Ag(1)−Se(4)	116.00(6)
Se(5)−Ag(1)−Se(3)	121.08(6)	Se(4)−Ag(1)−Se(3)	97.93(5)
Se(5)−Ag(1)−Se(6)	96.68(5)	Se(4)−Ag(1)−Se(6)	115.93(6)
Se(3)−Ag(1)−Se(6)	110.31(5)	Se(5)−Ag(1)−W(1)	142.66(5)
Se(4)−Ag(1)−W(1)	49.11(3)	Se(3)−Ag(1)−W(1)	49.37(3)
Se(6)−Ag(1)−W(1)	120.66(5)	Se(5)−Ag(1)−W(2)	48.50(4)
Se(4)−Ag(1)−W(2)	137.91(5)	Se(3)−Ag(1)−W(2)	123.88(5)
Se(6)−Ag(1)−W(2)	48.88(3)	W(1)−Ag(1)−W(2)	167.60(4)
Se(8)−Ag(2)−Se(9)	109.33(6)	Se(8)−Ag(2)−Se(6)	96.93(5)
Se(9)−Ag(2)−Se(6)	125.76(6)	Se(8)−Ag(2)−Se(10)	126.65(6)
Se(9)−Ag(2)−Se(10)	96.94(5)	Se(6)−Ag(2)−Se(10)	104.09(5)
Se(8)−Ag(2)−W(2)	48.11(3)	Se(9)−Ag(2)−W(2)	130.41(5)
Se(6)−Ag(2)−W(2)	48.98(3)	Se(10)−Ag(2)−W(2)	132.52(5)
Se(8)−Ag(2)−W(3)	131.88(5)	Se(9)−Ag(2)−W(3)	48.09(3)
Se(6)−Ag(2)−W(3)	131.14(5)	Se(10)−Ag(2)−W(3)	48.95(3)
W(2)−Ag(2)−W(3)	178.47(5)	Se(11)[b]−Ag(3)−Se(10)[b]	97.67(6)
Se(11)[b]−Ag(3)−Se(3)	111.72(6)	Se(10)[b]−Ag(3)−Se(3)	120.08(6)
Se(11)[b]−Ag(3)−Se(2)	126.54(7)	Se(10)[b]−Ag(3)−Se(2)	110.21(6)
Se(3)−Ag(3)−Se(2)	92.71(6)	Se(11)[b]−Ag(3)−W(1)	151.54(5)
Se(10)[b]−Ag(3)−W(1)	110.32(5)	Se(3)−Ag(3)−W(1)	49.50(3)
Se(2)−Ag(3)−W(1)	48.21(4)	Se(11)[b]−Ag(3)−W(3)[b]	48.91(4)
Se(10)[b]−Ag(3)−W(3)[b]	49.35(3)	Se(3)−Ag(3)−W(3)[b]	137.59(6)
Se(2)−Ag(3)−W(3)[b]	129.61(6)	W(1)−Ag(3)−W(3)[b]	159.51(4)
W(1)−Se(2)−Ag(3)	71.87(5)	W(1)−Se(3)−Ag(3)	72.29(5)
W(1)−Se(3)−Ag(1)	72.47(4)	Ag(3)−Se(3)−Ag(1)	95.77(5)
W(1)−Se(4)−Ag(1)	74.04(4)	W(2)−Se(5)−Ag(1)	75.56(5)
W(2)−Se(6)−Ag(2)	73.92(4)	W(2)−Se(6)−Ag(1)	73.39(4)
Ag(2)−Se(6)−Ag(1)	101.24(5)	W(2)−Se(8)−Ag(2)	75.00(4)
W(3)−Se(9)−Ag(2)	74.78(5)	W(3)−Se(10)−Ag(3)[a]	73.17(4)
W(3)−Se(10)−Ag(2)	73.89(4)	Ag(3)[a]−Se(10)−Ag(2)	103.51(6)
W(3)−Se(11)−Ag(3)[a]	75.14(4)		

[a] Symmetry transformations used to generate equivalent atoms: (a) $x - {}^1/_2, -y + {}^1/_2, z - {}^1/_2$; (b) $x + {}^1/_2, -y + {}^1/_2, z + {}^1/_2$.

mutually linked by bridging cyanide ligands, thus forming a polymeric three-dimensional anion of basic formula $\{[(\mu_4\text{-}WSe_4)Cu_4(CN)_4]^{2-}\}_\infty$. Different from the analogous polymeric structure of $[WS_4(CuSCN)_4]^{2-}{}_\infty$ with bridging thiocyanate groups,[12d] in which great deviations of Cu−NCS and Cu−SCN angles cause the overall arrangement to show no directionality. The polymeric anions bridged by the cyanide are slightly bent with angles of Cu−C−N = 175.6(9)° and Cu−N−C = 174.5(10)°; the corresponding cyanide ligands act as nearly linear bridges between Cu atoms of the next WSe_4Cu_4 unit, and thus a cross-framework configuration is formed. The overall array shows a relatively special directionality, though no particular layer is displayed. The C−N bond length of 1.16(2) Å is identical to most other gaseous cyanides.[31] The Cu−C distance is slightly shorter than the Cu−N distance, together with N−Cu−N(#) angle of 110.0(5)° being smaller than the C−Cu−C(#) angle of 115.6(6)°, suggesting that the Cu−C bond is stronger than the Cu−N bond.[32] Owing to cluster anion packing along the *b* axis (Figure 4), the WSe_4Cu_4 unit is bridged by cyanide ligands extending along the *c* axis, giving rise to three-dimensional channels running down the crystallographic *c* axis. These channels provide cavities of sufficient size for $[Et_4N]^+$ cations, which appear to precipitate the polymeric structure and presum-

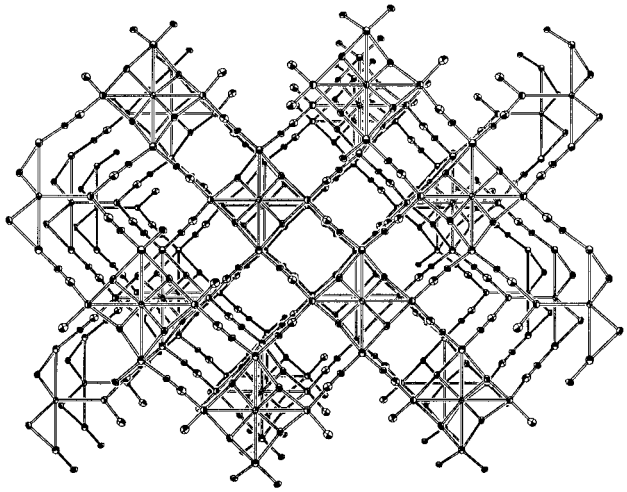

Figure 3. View of the three-dimensional cross-framework of the $[(\mu_4\text{-}WSe_4)Cu_4(CN)_4]^{2-}{}_\infty$ anion along the *a* axis with the ellipsoids drawn at the 50% probability level.

Table 3. Selected Bond Distances and Angles in **4**[a]

Bond Distances (Å)			
W−Se	2.3383(10)	W−Cu(1)	2.850(2)
W−Cu(2)	2.907(2)	Cu(1)−Se	2.4372(14)
Cu(2)−Se	2.4677(15)	Cu(1)−N(1)	1.987(10)
Cu(2)−C(1)	1.943(10)	C(1)−N(1)	1.160(13)

Bond Angles (deg)			
Se−W−Se	108.80(5)	Se−W−Se(#1)	109.68(5)
Se−W−Cu(1)	125.03(2)	Se−W−Cu(#1)	54.97(2)
Cu(1)−W−Cu(#1)	180.0	Se−W−Cu(2)	54.84(3)
Se−W−Cu(#2)	125.16(3)	Cu(1)−W−Cu(2)	90.0
Cu(2)−W−Cu(#2)	180.0	W−Se−Cu(1)	73.26(4)
W−Se−Cu(2)	74.38(4)	Cu(1)−Se−Cu(2)	112.20(5)
N(1)−Cu(1)−N(#1)	110.0(5)	N(1)−Cu(1)−Se	109.9(3)
N(1)−Cu(1)−Se	111.7(3)	Se−Cu(1)−Se	103.55(8)
N(1)−Cu(1)−W	125.0(3)	Se−Cu(1)−W	51.77(4)
C(1)−Cu(2)−C(#1)	115.6(6)	C(1)−Cu(2)−Se	112.3(3)
C(1)−Cu(#2)−Se	107.1(3)	Se−Cu(2)−Se	101.55(8)
C(1)−Cu(2)−W	122.2(3)	Se−Cu(2)−W	50.77(4)
C(1)−N(1)−Cu(1)	174.5(10)	N(1)−C(1)−Cu(2)	175.6(9)

[a] #1, $-x - {}^5/_4, -y, -z + {}^3/_4$; #2, $-x - {}^5/_4, -y - {}^1/_4, z$.

(31) Britton, D. *Perspect. Struct. Chem*. **1967**, *1*, 109.
(32) Bouslama, L.; Daoudi, A.; Mestagh, H.; Suard, M. *J. Mol. Struct. (THEOCHEM)* **1995**, *330*, 187.

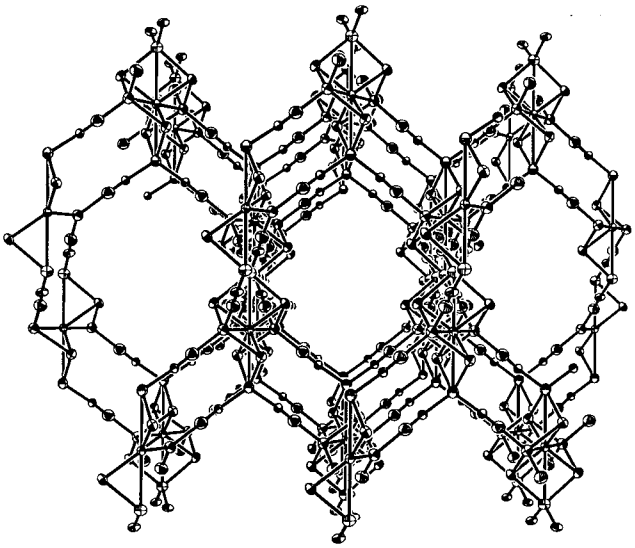

Figure 4. Perspective view of the three-dimensional network, running along the *b* axis in the $[(\mu_4\text{-}WSe_4)Cu_4(CN)_4]^{2-}{}_\infty$ anion.

ably help to balance the cluster anions. The diameter of the inner cavities is ca. 13 Å. The distance between the nearest Cu atoms is 4.071 Å.

Cyanide-bridged polymeric metal complexes are ubiquitous because cyanide as a conjugated bridging ligand is capable of linkage isomerization. However, those having heterometallic polymeric structures are rather uncommon. Moreover, polymeric clusters containing $[MQ_4]^{2-}$ (M = Mo, W; Q = S, Se) groups are very rare. Organotin−cyanometalate coordination polymers $\{[M(CN)_6]_2(R_2Sn)_3\}_n$ (M = Co, Fe; R = Et, ^{i}Pr, and ^{t}Bu) formed by $[M(CN)_6]^{3-}$ anions with $[R_2Sn]^{2+}$ cations have the same framework topology.[33] The cluster structure of $\{[(\eta^5\text{-}C_5Me_5)WS_3]_2Ag_3(CN)\}_n$ was reported to have an intriguing helical polymeric arrangement.[11h] To our knowledge, the only example of a cyanide-bridged polymeric cluster containing the $[MoS_4]^{2-}$ anion is the CuCN adduct of thiomolybdate $\{[Me_4N]_2[MoS_4(CuCN)_2]\}_n$, which has a polymeric structure that consists of an infinite zigzag chain of $(CuCN)_\infty$.[12a]

Thermal Stability. The present polymeric clusters **1**, **2**, and **4** show remarkable thermal stability. Thermal gravimetric analysis for **1** showed no weight loss up to 352 °C. From this point to 461 °C the lost weight fraction is 35.6%, which corresponds reasonably well to the lost organic composition (the theoretical value for $Ph_4P/[Ph_4P][WSe_4Ag]$ is 35.8%). The cluster **2** shows a similar thermal behavior with a weight loss occurring at 188 °C; this value is close to the boiling point of Me_2SO solvent. Losing weight for cluster **4** under heating occurs at 255 °C and closes at 348 °C in a measuring range from 20 to 800 °C.

NLO Properties. The nonlinear optical (NLO) properties of **2** and **4** were investigated. According to our previous studies on the third-order NLO properties of heterobimetallic sulfuric clusters, structure alternation and the skeleton atom substitute can induce larger changes in the NLO properties. Cubane-like clusters, hexagonal prism-shaped clusters, twin-nest-shaped cluster, twenty-nuclear supracage-shaped clusters, and linear chain clusters have relatively strong nonlinear optical absorption and refraction.[34] The pentanuclear "open" structural cluster $[WS_4Cu_4(SCN)_2(Py)_6]$ and hexagonal prism-shaped cluster $[Mo_2Ag_4S_8(AsPh_3)_4]$ have strong optical limiting effects.[35] Moreover, a significant improvement of optical absorptions and limiting capability is found when skeleton Cu and Mo atoms in clusters are replaced by Ag and W atoms, respectively. Thus, two silver clusters $[n\text{-}Bu_4N]_3[WAg_3S_4Br_3]$ and $[W_2Ag_4S_8(AsPh_3)_4]$ are proved to be the cluster materials with the better NLO properties. Recently we have found that the cluster $[(\mu_4\text{-}WSe_4)Cu_4(\mu\text{-dppm})_4]$ with a planar WCu_4 core has large optical limiting effects with a limiting threshold of 0.3 J·cm^{-2},[30b] and the cubane-like cluster $[(\mu_3\text{-}MoSe_4)Ag_3(PPh_3)_3Cl]$ shows very good nonlinear absorption and a strong optical response effect.[36] In this text studies on NLO properties of one-dimensional chain cluster **2** and three-dimensional framework cluster **4** are expected to expand inorganic cluster nonlinear optics.

Cluster **2** exhibits both NLO absorption and NLO refraction properties. The NLO absorption component was evaluated with *Z*-scan data obtained under an open aperture configuration, as shown in Figure 5. Theoretical curves of light transmittance against the *Z*-position of the sample were calculated according to eqs 1 and 2, using experimentally measured values of α_0, *L*,

$$T(Z) = \frac{1}{\pi^{1/2} q(Z)} \int_{-\infty}^{\infty} \ln[1 + q(z)] e^{-\tau^2} \, d\tau \qquad (1)$$

$$q(Z) = \alpha_2 I_i(Z) \frac{(1 - e^{-\alpha_0 L})}{\alpha_0} \qquad (2)$$

and $I_i(z)$ and using the effective nonlinear absorption coefficient, α_2, as an adjustable parameter. The dotted line shown in Figure 5 is the one that fit best to the *Z*-scan data observed. The curve corresponds to an α_2 value of 2.2×10^{-9} m·W^{-1}. The NLO refractive component of **2** was assessed by dividing the normalized *Z*-scan data obtained under the closed aperture configuration by the data obtained under open aperture configuration, which is plotted in Figure 6. The valley/peak pattern of the normalized transmittance curve shows the characteristic self-focusing behavior of the propagating light in the sample. The n_2 value was estimated from these data to be 6.8×10^{-15} m^2·W^{-1}. The discrepancy between the experimental and the theoretical values indicates involvement of higher-order NLO processes that are known to have a tendency to result in steep *Z*-scan curves.[37]

The optical limiting effects of clusters **2** and **4** are depicted in Figure 6. The linear and nonlinear transmission data of 0.13 mM in DMF for **2** and 0.09 mM in DMF for **4** were measured at 532 nm with 7 ns pulses produced by a frequency-doubled Q-switched Nd:YAG laser. Within a limited number of series cubane-like and defective-cubane clusters where both Ag- and Cu-containing clusters are measured and hence a comparison

(33) (a) Lu, J.; Harrison, W. T. A.; Jacobson, A. J. *Inorg. Chem*. **1996**, *35*, 4271. (b) Niu, T.-Y.; Lu, J.; Wang, X.-Q.; Korp, J. D.; Jacobson, A. J. *Inorg. Chem*. **1998**, *37*, 5324. (c) Siebel, E.; Ibrahim, A. M. A.; Fischer, R. D. *Inorg. Chem*. **1999**, *38*, 2530.

(34) (a) Shi, S.; Ji, W.; Lang, J.-P.; Xin, X.-Q. *J. Phys. Chem*. **1994**, *98*, 3570. (b) Hoggard, P. E.; Hou, H.-W.; Xin, X.-Q.; Shi, S. *Chem. Mater*. **1996**, *8*, 2218. (c) Sakane, G.; Shibahara, T.; Hou, H.-W.; Xin, X.-Q.; Shi, S. *Inorg. Chem.* **1995**, *34*, 5363. (d) Hou, H.-W.; Xin, X.-Q.; Liu, J.; Chen, M.-Q.; Shi, S. *J. Chem. Soc., Dalton Trans.* **1994**, 3211. (e) Hou, H.-W.; Liang, P.; Xin, X.-Q.; Yu, K. B.; Ge, P.; Ji, W.; Shi, S. *J. Chem. Soc., Faraday Trans.* **1996**, *92*, 2343. (f) Shi, S.; Ji, W.; Xin, X.-Q. *J. Phys. Chem*. **1995**, *99*, 894. (g) Lang, J.-P.; Tatsumi, K.; Kawaguchi, H.; Lu, J.-M.; Ge, P.; Ji, W.; Shi, S. *Inorg. Chem*. **1996**, *35*, 7924.

(35) (a) Low, M. K. M.; Hou, H.-W.; Zheng, H.-G.; Wong, W.-T.; Jin, G.-X.; Xin, X.-Q.; Ji, W. *Chem. Commun. (Cambridge)* **1998**, 505. (b) Ji, W.; Shi, S.; Du, H.-J.; Ge, P.; Tang, S.-H.; Xin, X.-Q. *J. Phys. Chem*. **1995**, *99*, 17297.

(36) Zhang, Q.-F.; Xin, X.-Q.; Xiong, Y.-N.; Ji, W. Submitted for publication.

(37) (a) Stegeman, G. L.; Torruellas, W. *Mater. Res. Soc. Symp. Proc*. **1994**, *328*, 397. (b) Mealli, C.; Proserpio, D. M. *J. Chem. Educ*. **1990**, *26*, 399.

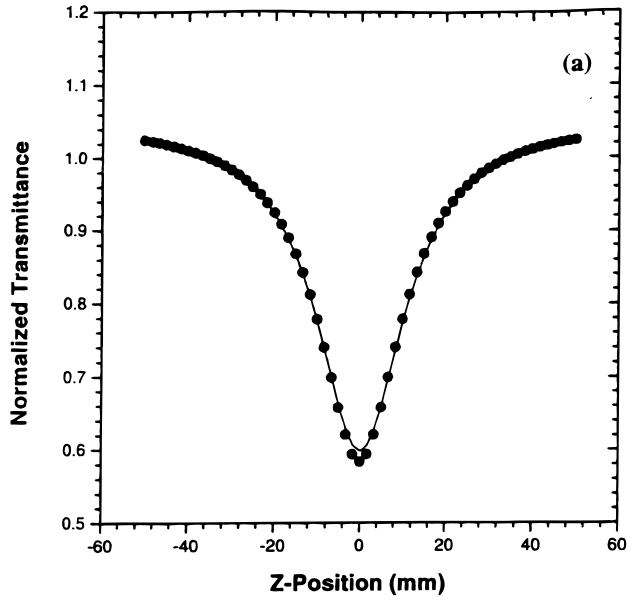

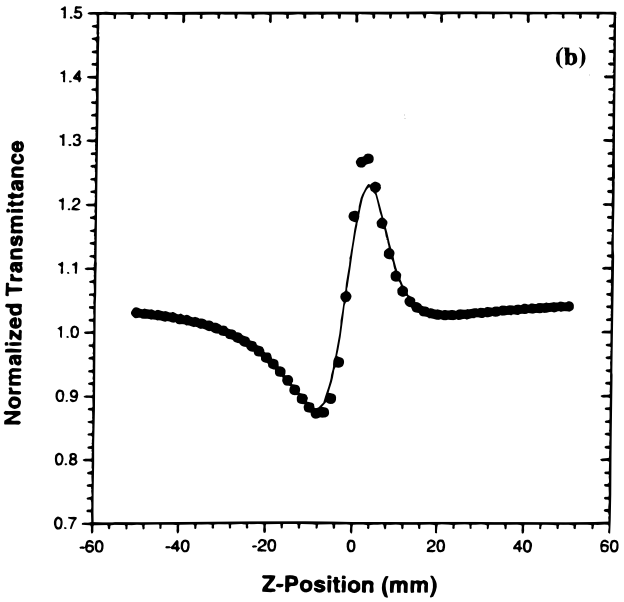

Figure 5. *Z*-scan data (filled circles) of 1.3×10^{-4} M $\{[La(Me_2SO)_8][(\mu\text{-}WSe_4)_3Ag_3]\}_n$ **2**, at 532 nm with $I(Z = 0)$ being 1.2×10^{12} W·m^{-2}. (a) Collected under an open aperture configuration showing NLO absorption. The solid curve is a theoretical fit based on eqs 1 and 2. (b) Obtained by dividing the normalized *Z*-scan data obtained under a closed aperture configuration by the normalized *Z*-scan data in part a. It shows self-focusing effect of the cluster.

can be made, the Ag-containing clusters seem always to outperform their corresponding Cu-containing counterparts in optical limiting at a given wavelength.[38] However, the present two polymeric clusters, which have an entirely different kind of structural type, show a result that the optical limiting capability of the WCu_4 core planar framework cluster is obviously better than that of a W/Ag helical chain cluster. At very low fluences they respond linearly to the incident light obeying Beer's law. For **2**, the light energy transmitted starts to deviate from Beer's law as the input light fluence reaches about 0.5 J·cm^{-2}, and the solution becomes increasingly less transparent as the fluence rises. The limiting threshold was

(38) Long, D.-L.; Shi, S.; Xin, X.-Q.; Luo, B.-S.; Chen, L.-R.; Huang, X.-Y.; Kang, B.-S. *J. Chem. Soc., Dalton Trans.* **1996**, 2617.

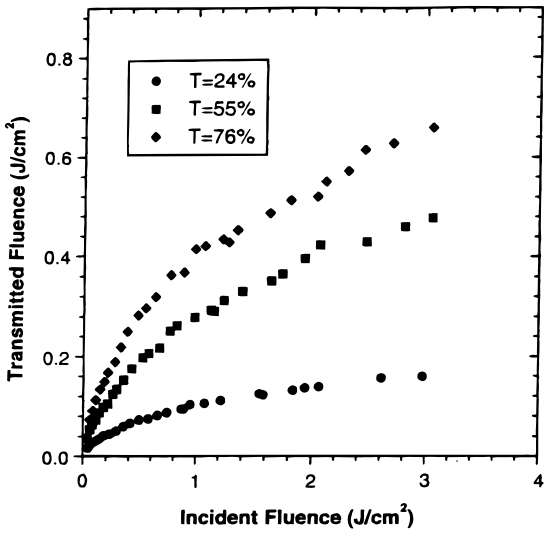

Figure 6. Optical limiting effect of $\{[La(Me_2SO)_8][(\mu\text{-}WSe_4)_3Ag_3]\}_n$ **2** (1.3×10^{-4} M in DMF, ■), $\{[Et_4N]_2[(\mu_4\text{-}WSe_4)Cu_4(CN)_4]\}_n$ **4** (0.9×10^{-4} M in DMF, ●), and C_{60} (6.4×10^{-4} M in toluene, ◆).

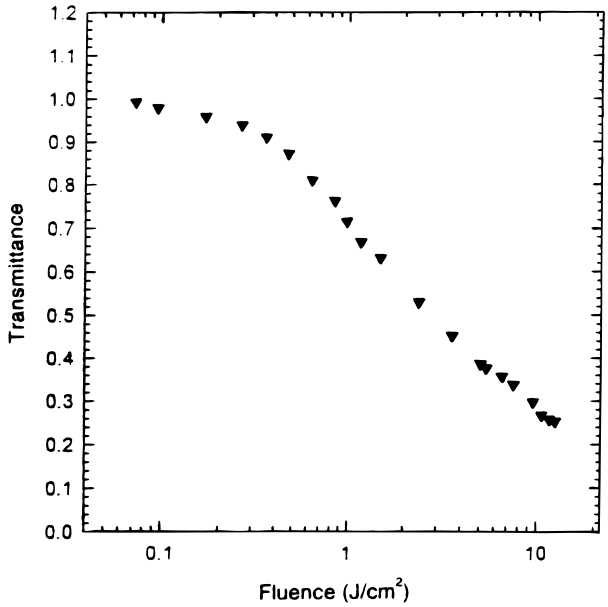

Figure 7. Energy dependent transmittance of a $\{[Et_4N]_2[(\mu_4\text{-}WSe_4)\text{-}Cu_4(CN)_4]\}_n$ DMF solution (0.9×10^{-4} M). Optical path: 1 mm. Laser wavelength: 532 nm. Pulse duration: 7 ns. Repetition rate: single shots (30 s interval).

measured as 0.7 J·cm^{-2} with a saturation fluence transmitted of ca. 2.5 J·cm^{-2}. An ideal optical-limiting material should be able to respond quickly to the incident light and become increasingly opaque as the incident fluence increases. Interestingly, for **4**, the solution transmittance is independent of the incident fluence at <0.1 J·cm^{-2}. When the incident fluence exceeds 0.1 J·cm^{-2}, the solution transmittance decreases as the incident fluence is increased, thus exhibiting a typical optical limiting effect. The optical limiting performance with repetition rate at single shots (30 s interval) is also displayed in Figure 7, from which we determined the limiting threshold in DMF solution to be ca. 0.2 J·cm^{-2}. Within the experimental errors, no significant difference was found among the measurements, thereby indicating that the photostability of $\{[Et_4N]_2[(\mu_4\text{-}WSe_4)\text{-}Cu_4(CN)_4]\}_n$ is considerably better than that of other known optical limiting inorganic clusters. Further support for the stability of **4** arises from the fact that the sample remained

effective even if the sample was prepared several months ago. The optical limiting capability of the three-dimensional cross-framework cluster **4** is better than that of C_{60},[39] the planar WCu_4 core sulfuric cluster $[WS_4Cu_4(SCN)_2(Py)_6]$,[35a] and one-dimensional chain cluster **2** and is comparable to that of phthalocyanine derivatives[40] and hexagonal prism-shaped cluster $[Mo_2Ag_4S_8(AsPh_3)_4]$.[35b] Thus, attempts to exploit more versatile coordination geometries and structural types to achieve desired NLO functions should become an important task.

In summary, we have successfully synthesized and structurally characterized two typical silver and copper heteroselenometallic polymeric clusters containing tetraselenotungstate anion. The remarkable dependence of the produced polymeric clusters on the kind of different self-assembly reaction system is noteworthy. The silver polymeric cluster **2** exhibits both strong optical absorption and optical self-focusing effect, while copper polymeric cluster **4** shows good photostability and a large optical limiting effect. Different from organic polymers, both polymeric clusters are constructed by hetero-metal atoms and semiconductor selenium atom; furthermore, they exhibit very special NLO properties. Further studies are in progress, which are directed toward the preparations of polymeric clusters having more versatile coordination geometries and novel structure types. Therefore, we shall try to design and synthesize new heteroselenometallic clusters whose structures and optical properties can be predicted and controlled.

Acknowledgment. This project was supported by the National Science Foundation (No. 296311040) of China and the Croucher Foundation of Hong Kong. We gratefully thank the Malaysian Government and Universiti Sains Malaysia for Research Grant R&D No. 190-9609-2801. We are indebted to Dr. Y. L. Song for NLO determinations and Dr. S. Shi for helpful discussions on NLO properties.

Supporting Information Available: X-ray crystallographic files in CIF format for clusters **2** and **4**. This material is available free of charge via the Internet at http://pubs.acs.org.

IC990780G

(39) McLean, D. G.; Sutherland, R. L.; Brant, M. C.; Brandelik, D. M.; Fleitz, P. A.; Pottenger, T. *Opt. Lett.* **1993**, *18*, 858.
(40) Perry, J. W.; Mansour, K.; Marder, S. R.; Perry, K. J.; Alvarez, D., Jr.; Choong, I. *Opt. Lett*. **1994**, *19*, 625.